



0016-7037(94)00343-2

Algorithms for the estimation of phase stability in heterogeneous thermodynamic systems

MARK S. GHIORSO

Department of Geological Sciences, University of Washington, Seattle, WA 98195, USA

(Received February 4, 1994; accepted in revised form June 13, 1994)

Abstract—Two critical aspects of the computation of equilibrium phase relations in highly nonideal thermodynamic systems are discussed: (1) identification of the saturation conditions and likely compositions of a suite of phases relative to a pervasive fluid phase, and (2) detection of phase separation within a homogeneous phase and estimation of compositions in the resulting equilibrium multiphase assemblage. New algorithms are described which address both of these problems in multicomponent thermodynamic systems and numerical results are presented for two and three component cases. An appendix illustrates a method of deriving analytical expressions for derivatives of the Gibbs free energies of phases characterized by internal “ordering” parameters.

INTRODUCTION

EQUILIBRIUM PHASE relations in multicomponent thermodynamic systems are usually computed by solving sequentially three interdependent subproblems. Initially, an estimate must be made of the identity, proportions, and compositions of phases in the system. Secondly, this estimate must be refined, in order to satisfy exactly the equilibrium condition for the specific set of imposed constraints, e.g., minimize the Gibbs free energy under the constraint of constant temperature, pressure, and system bulk composition. Thirdly, the resulting assemblage must be evaluated for potential metastability; derived phase compositions must fall outside miscibility gaps and phases not included in the system must be less stable than those currently in the equilibrium assemblage. This three-stage problem is solved iteratively and is the basis of modern computer algorithms for the computation of chemical equilibria in geochemical systems (SMITH and MISEN, 1982). If the phases in the system are ideal or approximately ideal, then the first and third stages of the calculation are straightforward and attention may be focused on the numerical problem of refining the equilibrium state from the initial guess. Historically, this problem has received the greatest attention, and for geochemical systems, the usual method of solution is some form of potential minimization. When attempts are made to calculate equilibrium relations in systems containing highly nonideal phases, more attention must be directed at the first and third stages of the calculation. Indeed, the most difficult and time-consuming aspect of the entire calculation can be establishing an initial guess of phase compositions and proportions for the potential minimization procedure. This paper presents two algorithms designed to rapidly estimate equilibrium phase compositions in geochemical systems dominated by highly nonideal phases. Specifically, methods are presented for (1) the determination of the saturation condition and composition of a phase in a system containing a pervasive fluid phase and (2) the detection of phase separation within a homogeneous phase and estimation of the compositions of the resulting multiphase assemblage. These algorithms are incorporated into the MELTS software package (GHIORSO and SACK, 1994) which models chemical equilibria in magmatic systems. They should

however, be equally applicable to systems dominated by an aqueous or gas phase, and may find use in modeling water/rock interaction or the vapor sublimation of solids.

This paper is organized into three logical sections. The phase stability algorithm is discussed in the first and the phase separation algorithm is outlined in the second. Implementation of either algorithm depends on the ability to evaluate analytically, first and second order compositional derivatives of the Gibbs free energy of any phase in the system. The final section of the paper (provided as an appendix) describes a method of obtaining these derivatives for solution models parameterized in terms of both compositional and ordering variables. Such formulations are typically invoked to model the Gibbs free energies of solid solutions with temperature, pressure, and composition dependent cation ordering.

Estimation of Phase Stability in Thermodynamic Systems with a Fluid Phase

Consider a thermodynamic system of p -components which has at least one p -component phase. For context, one might imagine a magmatic system containing a molten silicate liquid. Let us investigate the problem of determining the saturation condition of a solid phase, with respect to a particular bulk composition of this liquid, at certain specified values of temperature (T) and pressure (P). Specifically, we seek a quantitative estimate of the extent of under- or super-saturation of the solid with respect to the liquid, which implies, if the solid in question is itself a multicomponent solution, a determination of the composition of the solid which comes closest to being in equilibrium with this liquid at the specified T and P . This problem has an elegant geometrical solution and is easy to visualize in a two-component system.

In Fig. 1, we plot hypothetical Gibbs free energy surfaces for a two-component liquid (dark gray) and solid (white) at three saturation conditions. A tangent plane to the liquid Gibbs surface is also indicated. Its point of tangency corresponds to an assumed liquid bulk composition. The solid is undersaturated with respect to the liquid if its Gibbs surface is always above this tangent plane (Fig. 1a), supersaturated if it plunges below this plane (Fig. 1c), and at saturation if the tangent plane intersects the solid surface at one and only

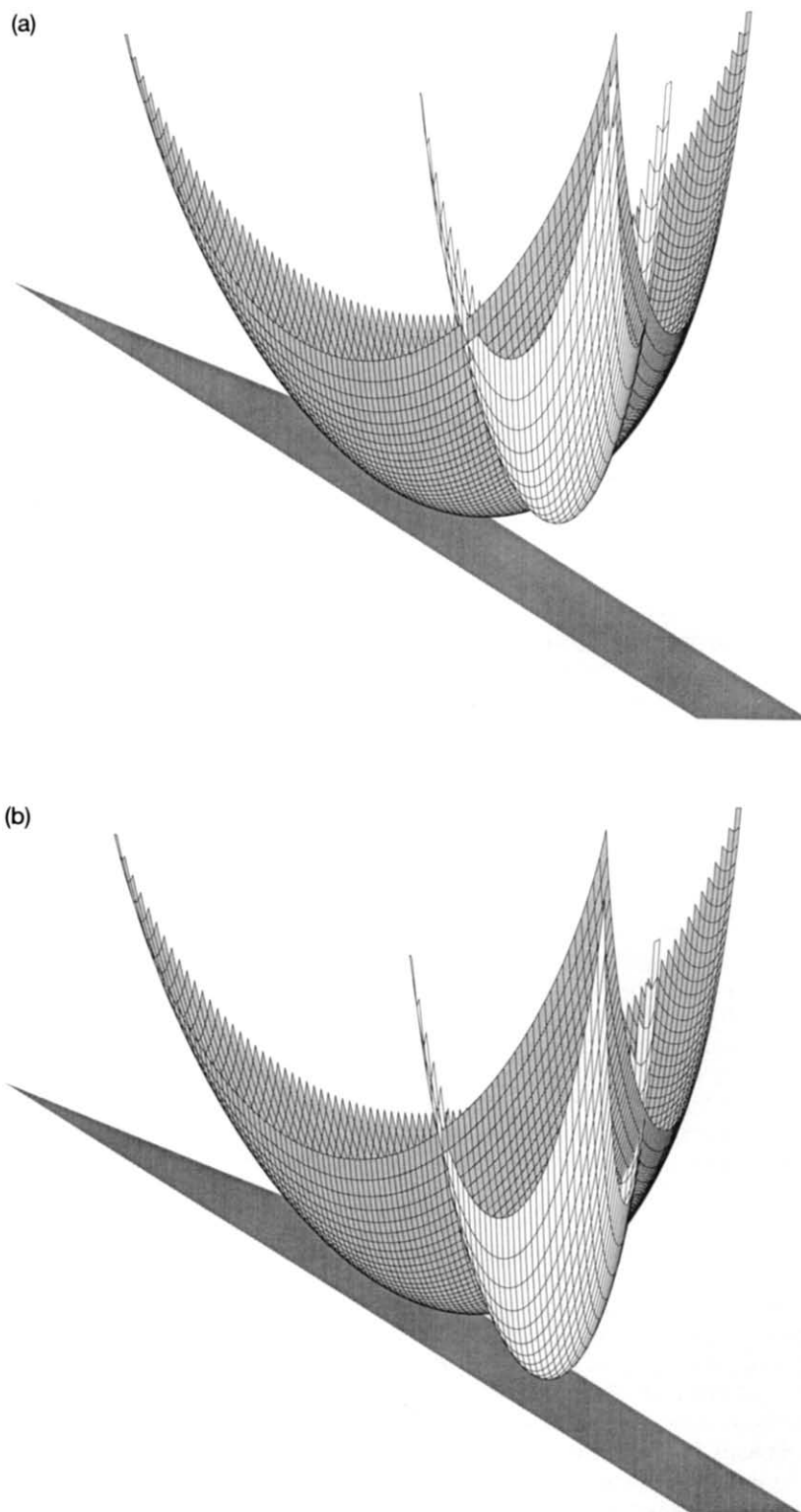


FIG. 1. Sketch of the molar Gibbs free energy surfaces of two phases in a two-component system. The vertical axis measures the Gibbs free energy of the system, while the horizontal axes, in and out of the page, describe compositional variation. A plane is drawn tangent to the phase denoted by the gray-colored mesh surface at some specified reference composition. External conditions (i.e., T , P) are varied such that the second phase (denoted by the white-colored mesh surface) is undersaturated (a), saturated (b), and supersaturated (c), with respect to the first at this reference composition.

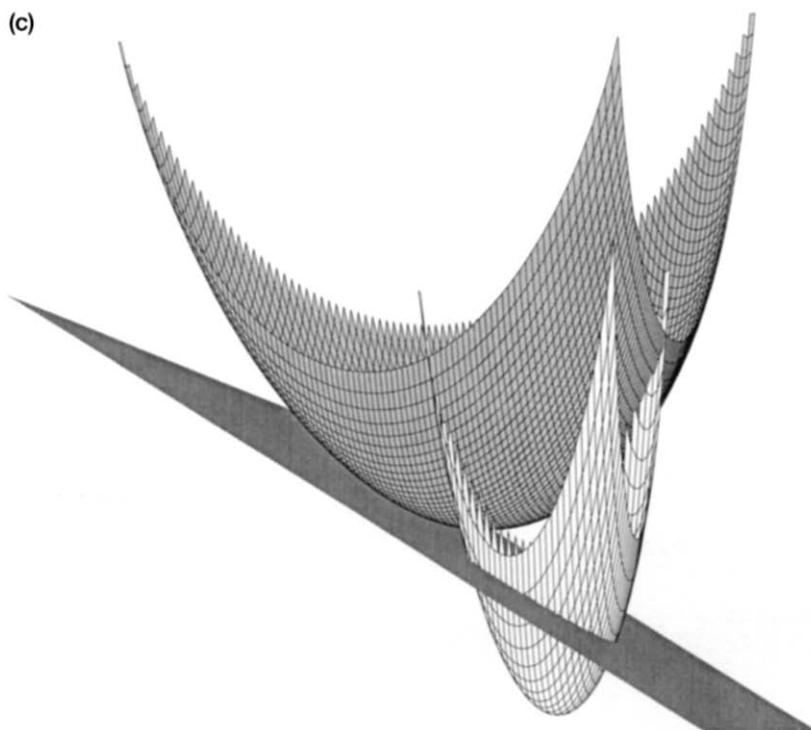
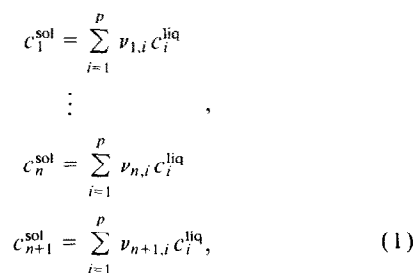


FIG. 1. (Continued)

one point (Fig. 1b). As a tangent plane to the Gibbs surface may be defined in terms of chemical potentials of components in the phase (DARKEN and GURRY, 1953), the last diagram is nothing more than a visualization of the condition of the equality of chemical potentials in all phases in a system at thermodynamic equilibrium. If, for the undersaturated (Fig. 1a) or supersaturated (Fig. 1c) states, one imagines a tangent plane to the solid surface which is parallel to the tangent plane of the liquid, then the point of tangency of this plane to the solid surface defines the composition of the solid "most nearly" or "closest" to equilibrium with the liquid. If we extend a vertical chord from the solid Gibbs surface at this particular composition until it touches the liquid tangent plane, the length of this chord is the chemical affinity: an energetic measure of the extent of under- or super-saturation. It follows that in a two-component system, the chemical affinity is nothing more than the offset between two mutually parallel tangent planes. For a thermodynamic system of more components, the principle is the same. A tangent hypersurface is extended from the liquid Gibbs surface at the bulk composition of the liquid and a particular solid composition is identified, such that a tangent hypersurface to the solid Gibbs surface at this composition is "parallel" to that of the liquid. The energetic offset between the two hypersurfaces is the chemical affinity. The algorithm proposed here performs this geometrical evaluation numerically.

We assume the composition of the liquid (or more generally the fluid) is described by p -thermodynamic components, identified by $c_1^{\text{liq}}, c_2^{\text{liq}}, \dots, c_p^{\text{liq}}$. The solid, whose saturation condition is to be determined, is defined in terms of $n+1$ components (for reasons which will become clear below), identified by $c_1^{\text{sol}}, c_2^{\text{sol}}, \dots, c_n^{\text{sol}}, c_{n+1}^{\text{sol}}$. In practice, due

to limitations in our ability to construct comprehensive models for mineral solid solutions, $n+1$ is often less than p . Dissolution of the solid into the liquid may be symbolized by the following set of chemical reactions



where the $\nu_{i,j}$ are stoichiometric reaction coefficients transforming solid to liquid components. The Gibbs free energy change (ΔG) for each of the reactions in Eqn. 1 may be written

$$\begin{aligned} -\Delta G_1 &= \sum_{i=1}^p \nu_{1,i} \mu_i^{\text{liq}} - \mu_1^{\text{sol}} \\ &\vdots \\ -\Delta G_n &= \sum_{i=1}^p \nu_{n,i} \mu_i^{\text{liq}} - \mu_n^{\text{sol}} \\ -\Delta G_{n+1} &= \sum_{i=1}^p \nu_{n+1,i} \mu_i^{\text{liq}} - \mu_{n+1}^{\text{sol}}, \end{aligned} \quad (2)$$

where μ_i^j refers to the chemical potential of the i^{th} component in the j^{th} phase. The left-hand sides of the system in Eqn. 2 are zero if the liquid is saturated in the solid. In general, the

individual ΔG_i s in Eqn. 2 may be replaced with the chemical affinity, A , if we specify that the composition of the solid be chosen to be the "nearest equilibrium" composition discussed in the previous paragraph. This follows from the requirement that the tangent hypersurface to the solid Gibbs energy at this particular composition must be parallel to that of the liquid. In other words, the energetic offset of the two hypersurfaces in each component direction (i.e., the ΔG_i s) must be identical (equal to A), otherwise, the hypersurfaces would not be parallel. With this stipulation, Eqn. 2 becomes

$$\begin{aligned} -A &= \sum_{i=1}^p \nu_{1,i} \mu_i^{\text{liq}} - \mu_1^{\text{sol}} \\ &\vdots \\ -A &= \sum_{i=1}^p \nu_{n,i} \mu_i^{\text{liq}} - \mu_n^{\text{sol}} \\ -A &= \sum_{i=1}^p \nu_{n+1,i} \mu_i^{\text{liq}} - \mu_{n+1}^{\text{sol}}, \end{aligned} \quad (3)$$

which may be rearranged to yield

$$\begin{aligned} 0 &= \mu_1^{\text{sol}} - A - \sum_{i=1}^p \nu_{1,i} \mu_i^{\text{liq}} \\ &\vdots \\ 0 &= \mu_n^{\text{sol}} - A - \sum_{i=1}^p \nu_{n,i} \mu_i^{\text{liq}} \\ 0 &= \mu_{n+1}^{\text{sol}} - A - \sum_{i=1}^p \nu_{n+1,i} \mu_i^{\text{liq}}. \end{aligned} \quad (4)$$

Finally, the system of equations in Eqn. 4 may be simplified using the following identities:

$$\begin{aligned} \mu_j &= \mu_j^0 + RT \ln a_j, \\ \Delta \mu_j &= \mu_j^{0,\text{sol}} - \sum_{i=1}^p \nu_{j,i} \mu_i^{\text{liq}}, \end{aligned}$$

where a_j is the activity of the j^{th} component, R is the gas constant, and the superscript zero refers to the standard state.* This results in

$$\begin{aligned} 0 &= RT \ln a_1^{\text{sol}} - A + \Delta \mu_1 \\ &\vdots \\ 0 &= RT \ln a_n^{\text{sol}} - A + \Delta \mu_n \\ 0 &= RT \ln a_{n+1}^{\text{sol}} - A + \Delta \mu_{n+1}, \end{aligned} \quad (5)$$

which is the mathematical embodiment of the geometrical construction illustrated in Fig. 1.

Equation 5 represents a system of $n + 1$ equations in $n + 1$ unknowns. The unknowns are the chemical affinity for the solid-liquid reaction and the n -independent compositional variables which when specified, define uniquely the activities of the $n + 1$ thermodynamic components. For example, we might choose the first n mole fractions (X) as

independent compositional variables. Utilizing the identity, $X_{n+1}^{\text{sol}} = 1 - X_1^{\text{sol}} - \dots - X_n^{\text{sol}}$, permits calculation of the $n + 1$ activity terms, and the set of unknowns in Eqn. 5 becomes $\{X_1^{\text{sol}}, \dots, X_n^{\text{sol}}, A\}$. In general, the composition of the solid may be specified by the set of parameters r_1, r_2, \dots, r_n , which may or may not correspond to the first n component mole fractions.

If the solid is an ideal solution, the system in Eqn. 5 has an analytical solution. Setting activity equal to mole fraction, we rewrite Eqn. 5 as

$$\begin{aligned} 0 &= RT \ln X_1^{\text{sol}} - A + \Delta \mu_1 \\ &\vdots \\ 0 &= RT \ln X_n^{\text{sol}} - A + \Delta \mu_n \\ 0 &= RT \ln (1 - X_1^{\text{sol}} - \dots - X_n^{\text{sol}}) - A + \Delta \mu_{n+1}. \end{aligned} \quad (6)$$

Subtracting the n^{th} equation from the rest eliminates the chemical affinity term and establishes a relation between the first $n - 1$ and the n^{th} mole fractions:

$$\begin{aligned} X_1^{\text{sol}} &= \beta_1 X_n^{\text{sol}} \\ &\vdots \\ X_{n-1}^{\text{sol}} &= \beta_{n-1} X_n^{\text{sol}}, \end{aligned} \quad (7)$$

and

$$X_n^{\text{sol}} = \beta_n (1 - X_1^{\text{sol}} - \dots - X_n^{\text{sol}}), \quad (8)$$

where the constants β_i are given by

$$\begin{aligned} \beta_1 &= e^{-(\Delta \mu_1 - \Delta \mu_n)/RT} \\ &\vdots \\ \beta_{n-1} &= e^{-(\Delta \mu_{n-1} - \Delta \mu_n)/RT} \\ \beta_n &= e^{-(\Delta \mu_n - \Delta \mu_{n+1})/RT}. \end{aligned}$$

Substitution of Eqn. 7 into Eqn. 8 results in a solution for X_n^{sol}

$$X_n^{\text{sol}} = \frac{\beta_n}{[1 + \beta_n(1 + \beta_1 + \dots + \beta_{n-1})]}. \quad (9)$$

Evaluation of Eqns. 9 and 7, along with any one of those in the system stipulated in Eqn. 6 provides a unique solution for the saturation condition in the case of an ideal solution.

For the general case of nonideal activity composition relations, the solution of the nonlinear system in Eqn. 5 is effected by forming the sum of squares of the right-hand-sides of the system, i.e.,

$$\Phi(r_1, \dots, r_n, A) = \sum_{i=1}^{n+1} (RT \ln a_i^{\text{sol}} - A + \Delta \mu_i)^2, \quad (10)$$

and minimizing this sum of squares with respect to the unknown affinity and composition variables. The numerical technique used in the following examples and suggested for general implementation is based upon a modification of Marquardt's procedure (NASH, 1990). The technique and modifications are discussed in the appendix. Unfortunately, finding the minimum of Eqn. 10 is fraught with difficulties. Most of the problems and the numerical tricks to work around them, can be illustrated using a simple two-component example.

* Here, defined as unit activity of the pure substance (endmember solid component) at any T and P .

Consider a two-component solid solution with activity composition relations given by a regular-solution model:

$$\begin{aligned} a_1^{\text{sol}} &= X \exp\left[\frac{W(1-X)^2}{RT}\right] \\ a_2^{\text{sol}} &= (1-X) \exp\left[\frac{WX^2}{RT}\right]. \end{aligned} \quad (11)$$

For illustration, we choose a regular solution parameter (W) of 20 kJ, a temperature of 1000 K, and values of $\Delta\mu_1$ and $\Delta\mu_2$ equal to 1 and 2 kJ, respectively. Substituting Eqn. 11 into Eqn. 10, permits construction of a plot of Φ as a function of X for a given value of A . In Fig. 2, we plot Φ vs. X for the regular solution model, adopting a value for A of -0.1 kJ. A similar curve for ideal activity-composition relations is also plotted and corresponds to a value of A of 4.3 kJ. These affinities were chosen in order to make Φ evaluate to zero somewhere in the interval $0 \leq X \leq 1$. They are the optimal; adopting other values cause Φ to be strictly greater than zero over this interval. An examination of Fig. 2 reveals that even though we have purposely chosen a very simple nonideal model for the activity-composition relations of this solid solution, this model generates multiple minima in Φ . The solution sought is the one with the deepest minimum, the so-called "global" minimum. The numerical algorithm used to minimize Eqn. 10 must find that minimum or the answer will not be physically realistic. Herein lies the problem. The minimum found by the algorithm will depend on the specified initial guess of its location. This is because all numerical methods aimed at this class of problems work by accepting some initial guess to the minimum, by computing a "downhill" search direction at that guess, and by proceeding in the indicated direction until the minimum is reached. These methods are intrinsically "local" and there is no way to know if the minimum found is the answer sought, without bringing

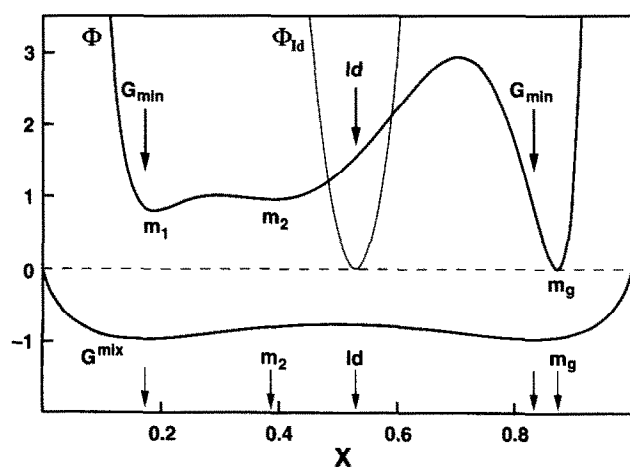


FIG. 2. Plot of (1) the molar Gibbs free energy of mixing (\bar{G}^{mix}) of a two-component regular solution (W equal 20 kJ, T equal 1000 K), (2) the function Φ (Eqn. 10) for this solution ($\Delta\mu_1$ equal 1 kJ, $\Delta\mu_2$ equal 2 kJ), and (3) a function Φ for the corresponding ideal solution. The mole fraction (X) of the first component is plotted on the ordinate. The arrows labeled G_{min} denote the minima in \bar{G}^{mix} , that labeled Id denotes the minimum in Φ_{id} , and those labeled m_1 , m_2 , and m_g refer to minima in Φ .

to the method additional information regarding the nature of the global minimum. In the case of the function Φ we know that the global minimum has a function value of zero, and therefore have a criteria for identifying false solutions. What is needed, is a procedure to compute insightful initial guesses.

Examining Fig. 2, it may seem quite obvious how to proceed. Simply choose an initial guess to the right of the hump in the function that occurs at an X value of approximately 0.7. Of course, that is the logical way to proceed, but it is not a sufficiently general approach to be applicable to higher dimensional problems or those with more complex Gibbs functions. We need a general and systematic algorithm. Consider the following approach. Choose as an initial guess for the nonlinear minimization algorithm, values of X and A which correspond to the solution for ideal activity-composition relations. This initial guess has two important advantages: (1) It can be computed uniquely for arbitrarily large systems, and (2) it can be computed analytically and therefore rapidly. The composition given by this solution is labeled by the arrow "Id" in Fig. 2. Fueled with this initial guess, the nonlinear minimization algorithm proceeds to the local minimum labeled by m_2 in Fig. 2. This is a false minimum, which is detectable because the function value (Φ) is nonzero at this composition. Now, the strategy is to guess where the global minimum in Φ is likely to be, since the "easy to compute" initial guess failed. Note that in Fig. 2, the additional local minimum in Φ (labeled m_1) and the global minimum (labeled m_g) are crudely associated with minima in the Gibbs energy of mixing function of the solid. Perhaps recomputing an initial guess corresponding to one of the minima in the solid Gibbs function (\bar{G}^{mix}) would be a better choice? Finding these minima in \bar{G}^{mix} is itself computationally costly, in that an iterative procedure must be used. However, the minimization of \bar{G}^{mix} is a one parameter (X) problem and fast numerical algorithms are available (see below). To find the minimum in \bar{G}^{mix} , the algorithm needs to start somewhere; it requires its own initial guess to get going. We choose X_{id} . The downhill direction leads to larger values and eventually to the X -value labeled G_{min} in Fig. 2. This value, along with the value of A_{id} determined previously, is used as an initial guess to minimize the function Φ . The global minimum at m_g is found successfully by the algorithm starting from this new guess. Will this procedure always work? It is apparent from Fig. 2 that the reason this sequence of trials succeeded in finding the global minimum is because the right-hand minimum in \bar{G}^{mix} was located and provided the new guess for location of the minimum in Φ . This is a direct consequence of the fact that X_{id} (the starting point in the search for G_{min}) is located to the right of the maximum in the \bar{G}^{mix} surface at 0.5. Suppose, for discussion, X_{id} happened to be slightly smaller than 0.5. Then the \bar{G}^{mix} minimization procedure would have led to the left minimum, and the Φ minimization procedure would have found m_1 . In this eventuality, one last attempt can be made to find the global minimum in Φ . Start once again from X_{id} to minimize \bar{G}^{mix} , but this time move in the uphill direction, past the maximum in \bar{G}^{mix} , to find the minimum located on the other side of this maximum. This procedure eventually results in the correct identification of m_g .

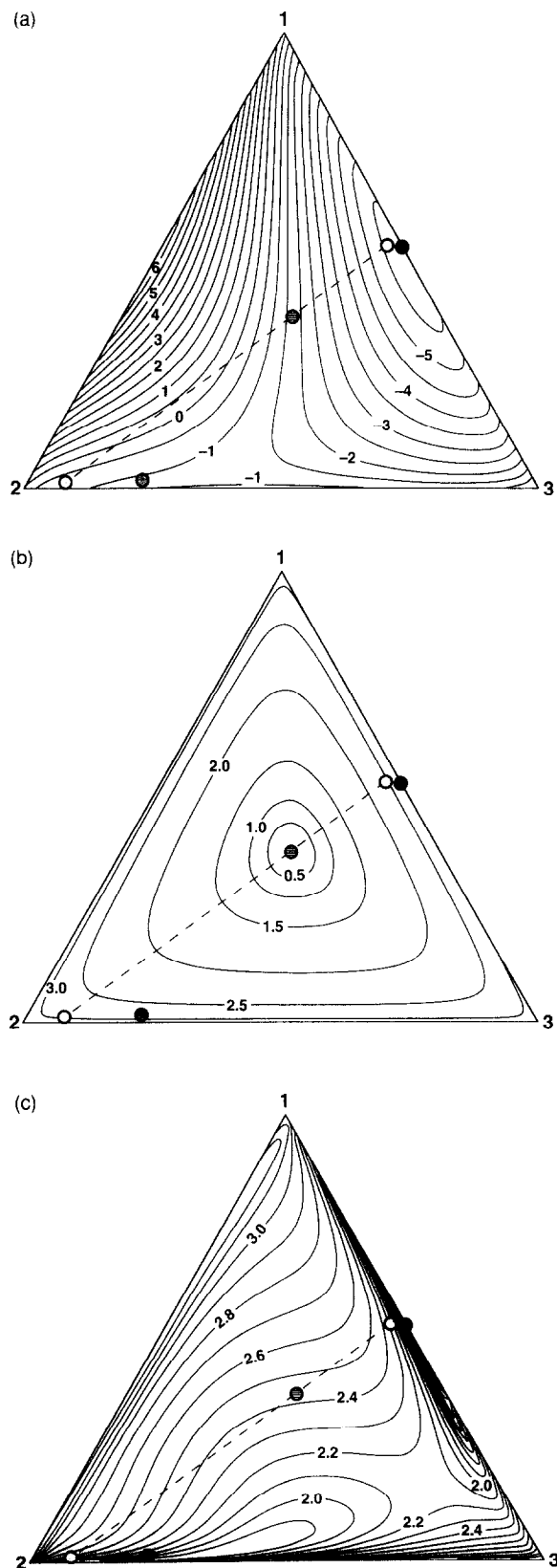


FIG. 3. Analysis of phase saturation conditions involving a three-component regular solution. H_{12} , H_{13} , and H_{23} are chosen to be 50, 0, and 20 kJ, respectively. $\Delta\mu_1$, $\Delta\mu_2$, and $\Delta\mu_3$ are taken as 1, 3, and 2 kJ. The temperature is assumed to be 1000 K. (a) Contour diagram, in kJ, of the molar Gibbs free energy of mixing (\bar{G}^{mix}). (b)

Having developed empirically an algorithmic strategy, suppose we try this procedure with a three-component solid. Consider a regular solution with H_{12} , H_{13} , and H_{23} equal to 50, 0, and 20 kJ, respectively. For the sake of illustration, we assume values of $\Delta\mu_1$, $\Delta\mu_2$, and $\Delta\mu_3$ of 1, 3, and 2 kJ. Figure 3a provides a contour map of the Gibbs free energy of mixing for this solution and Fig. 3b and c display contours of the logarithm of the Φ function assuming ideal mixing (3b), with an affinity of 7.174 kJ, and the regular solution model (3c), with an affinity of 4.326 kJ. As in the previous example, the affinity values chosen for plotting are optimal and allow Φ to have a value of zero somewhere in the ternary.

The global minimum in Φ is located very close to the 1–3 join and is indicated by the black dot in Fig. 3. The dot filled with horizontal rules denotes the position, $(X_1, X_2)_{\text{id}}$, of the minimum in Φ determined by assuming that the solid is an ideal solution. Figure 3b clearly shows this minimum in Φ_{id} . Following the procedure suggested above, $(X_1, X_2)_{\text{id}}$ is used as an initial guess to locate a minimum in Φ . It can be seen from Fig. 3c, that the downhill direction from this initial guess leads ultimately to the gray-filled dot which plots near the 2–3 join. This is a false minimum. A new initial guess needs to be computed. The procedure developed for the two-component case suggests returning to the point $(X_1, X_2)_{\text{id}}$ and proceeding from that point to the closest minimum in \bar{G}^{mix} . In the two-component case, that was an easy minimization problem in one parameter. In the present case, it is a multidimensional minimization problem, which is computationally costly and becomes progressively more difficult to solve as the number of components in the solid solution increases. Ideally, we would like to take advantage of the simplicity of the two-component minimization algorithm by searching within some pseudobinary section of this three-component system, performing a one parameter minimization along an optimally chosen search direction that most likely points towards minima in \bar{G}^{mix} . This pseudobinary section is given by the “direction of minimal curvature” of \bar{G}^{mix} , and corresponds to a vector which starts at $(X_1, X_2)_{\text{id}}$ and extends in the “most downhill” direction from that point. The direction of minimal curvature is provided by the minimum of a function (BARRON, 1978),

$$\rho(\vec{r}) = \frac{\vec{r}^T \left. \frac{\partial^2 \bar{G}^{\text{mix}}}{\partial \vec{r}^2} \right|_{\vec{r}_{\text{id}}} \vec{r}}{\vec{r}^T \vec{r}}, \quad (12)$$

known as the Rayleigh Quotient. In Eqn. 12, ρ is defined in terms of a scalar-valued function of a vector (\vec{r}) of concentration variables. In the three-component case being considered, \vec{r} is given by the vector $[X_1, X_2]$ and \vec{r}_{id} refers to the

Contour diagram of $\log(\Phi_{\text{id}})$ evaluated for an ideal three-component solution with $\Delta\mu_i$ as specified above. An affinity value of 7.174 kJ was used. (c) Contour diagram of $\log(\Phi)$ for the regular solution with $\Delta\mu_i$ as specified above. An affinity value of 4.326 kJ was used. In all three diagrams, the horizontally ruled dot denotes the minimum in Φ_{id} , the black dot the global minimum of Φ , the stippled dot a local minimum in Φ , and the open dots define minima in the \bar{G}^{mix} surface along the pseudobinary (dashed line) defined by the direction of minimal curvature of \bar{G}^{mix} at the point denoting the minimum of Φ_{id} .

point $(X_1, X_2)_{\text{ld}}$. Note that the second derivative matrix of \bar{G}^{mix} needs to be computed only at the point \bar{r}_{ld} . The minimum of ρ with respect to \bar{r} is given analytically by (NASH, 1990):

$$\left[\frac{\partial^2 \bar{G}^{\text{mix}}}{\partial \bar{r}^2} \right]_{\bar{r}_{\text{ld}}} \bar{r}_{\text{min}} = \rho_{\text{min}} \bar{r}_{\text{min}}. \quad (13)$$

Equation 13 may be recognized as a familiar eigenvector-eigenvalue problem. In order to minimize ρ , the particular solution of Eqn. 13 is sought that corresponds to the smallest eigenvalue (ρ_{min}) and its associated eigenvector (\bar{r}_{min}). For the three-component example under discussion here, the pseudobinary defined by \bar{r}_{min} is given by the dashed line in Fig. 3. We now initiate a one-dimensional search along this dashed line in order to minimize the projected Gibbs energy of mixing function:

$$\bar{G}^{\text{mix,proj}}(\bar{r}_{\text{ld}} + \lambda \bar{r}_{\text{min}}), \quad (14)$$

with respect to the free parameter, λ . Along this pseudobinary there are two minima in $\bar{G}^{\text{mix,proj}}$. These are indicated by the unfilled dots in Fig. 3. As in the two-component case, the one dimensional minimization algorithm proceeds downhill from $(X_1, X_2)_{\text{ld}}$ along this pseudobinary section and stops at the minimum closest to the 1–3 join. This then becomes the new initial guess and the global minimum in Φ is found directly. If the “downhill” search direction along the pseudobinary section had resulted in finding the other minimum of $\bar{G}^{\text{mix,proj}}$, the false minimum in Φ would have been attained, and the procedure would be to “look” uphill along the pseudobinary section until the maximum in $\bar{G}^{\text{mix,proj}}$ is crossed and the other minimum is achieved.

Based upon our analysis and the success of the previous examples, a general algorithmic scheme may be proposed.

Algorithm for the computation of the saturation state of a solid, referenced to a liquid of known composition, at some specified temperature and pressure

- (step 0a) Specify a model for the molar Gibbs free energy of mixing of an $n + 1$ component solid solution in terms of n independent compositional variables r_1, r_2, \dots, r_n (arranged as the elements of a vector, \bar{r}), T and P . Note that analytical expressions for the first and second compositional derivatives of this function (see appendix for general methods of obtaining these) are utilized here and are necessary for the specification of the chemical potentials of endmember components.
- (step 0b) For each endmember of the solid solution, compute the quantity $\Delta\mu$ as defined above. This will require specifying a reference bulk composition for the liquid phase, the availability of a model for computation of chemical potentials of components in the liquid, and the availability of thermodynamic data for the standard state properties of endmember solid components.
- (step 1) Solve Eqns. 8, 9, and 7 for $(X_1, X_2, \dots, X_n)_{\text{ld}}$ and transform the result (if a component transformation is necessary) into the reference point \bar{r}_{ld} . This is the solution to the problem assuming ideal mixing in the solid. Using the derived values of $(X_1, X_2, \dots, X_n)_{\text{ld}}$ and Eqn. 6 obtain

A_{ld} . If the “solid solution” has only one component (i.e., the saturation state for a pure endmember solid is in question), then exit the algorithm: A_{ld} gives the saturation condition. For the trivial case of an ideal solution model, the correct answer is also obtained at this step, and the algorithm should be exited.

- (step 2) Use \bar{r}_{ld} and A_{ld} as an initial guess to minimize the function Φ defined by Eqn. 10. Note that the solid activity terms in Eqn. 10 are entirely determined by specifying \bar{r} and the stipulated T and P . Minimize Φ using an algorithm based upon Marquardt’s method, which incorporates a mechanism for keeping the solution vector within feasible bounds (see Appendix and algorithm 23, *Modified Marquardt method for minimising a nonlinear sum-of-squares function*, of NASH, 1990).
- (step 3) Evaluate the function value of Φ at the minimum obtained in step 2. If Φ is zero, exit the algorithm.
- (step 4) Compute the direction of minimal curvature of \bar{G}^{mix} at \bar{r}_{ld} by minimizing the Rayleigh quotient given by Eqn. 12 using Algorithm No. 25 (*Rayleigh quotient minimisation by conjugate gradients*) of NASH (1990). This yields a unidirectional search vector (\bar{r}_{min}) which defines a pseudobinary section through \bar{G}^{mix} .
- (step 5) Minimize $\bar{G}^{\text{mix,proj}}$ (Eqn. 14) with respect to λ using Algorithm No. 17 (*Minimisation of a function of one variable*) of NASH (1990). Use \bar{r}_{ld} as an initial guess to the minimum of $\bar{G}^{\text{mix,proj}}$. Construct a new initial guess ($\bar{r}_{\text{ld}} + \lambda_{\text{min}} \bar{r}_{\text{min}}$) to the minimum of Φ from the result.
- (step 6) Utilizing the new initial guess computed in step 5, minimize Φ according to the method discussed in step 2.
- (step 7) Evaluate the function value of Φ at the minimum obtained in step 6. If Φ is zero, exit the algorithm.
- (step 8) Maximize $\bar{G}^{\text{mix,proj}}$ (Eqn. 14) with respect to λ by minimizing $-\bar{G}^{\text{mix,proj}}$ using the algorithm mentioned in step 5. Use \bar{r}_{ld} as an initial guess to the maximum of $\bar{G}^{\text{mix,proj}}$. This procedure results in λ_{max} .
- (step 9) Compute a new initial guess to the minimum of $\bar{G}^{\text{mix,proj}}$ as $\bar{r}_{\text{ld}} + (\lambda_{\text{max}} + \Delta\lambda) \bar{r}_{\text{min}}$, where $\Delta\lambda$ is a small number with the same sign as λ_{max} . Minimize $\bar{G}^{\text{mix,proj}}$ with respect to λ as in step 5. This results in a λ_{min} different than that obtained previously.
- (step 10) Use the value of λ_{min} obtained in step 9 to construct a new initial guess ($\bar{r}_{\text{ld}} + \lambda_{\text{min}} \bar{r}_{\text{min}}$) to the minimum of Φ .
- (step 11) Utilizing the new initial guess computed in step 10, minimize Φ according to the method discussed in step 2.
- (step 12) Evaluate the function value of Φ at the minimum obtained in step 11. If Φ is nonzero, report a failure of the algorithm.

In the software package MELTS (GHIORSO and SACK, 1994), the above algorithm is implemented in the C programming language and is used to solve problems involving solid phases with up to seven components coexisting with a twelve-component silicate liquid. As an additional complication, the solid solution models employed in MELTS generally involve internal “ordering” parameters which account for the energetic effects of composition, temperature, and pressure-dependent cation ordering. The procedure implemented in MELTS is highly successful in finding the global minimum in Φ and is used to calculate the onset of saturation

of a particular solid phase. This is effected by examining the sign of the chemical affinity which results from solution of the above algorithm. Positive affinities indicate undersaturation and negative affinities indicate supersaturation. When supersaturation is detected for a particular solid, that solid is added to the list of stable phases in the system with the composition indicated by the above algorithm. This composition is then refined and the mass of the precipitated solid calculated by direct minimization of the potential function which characterizes thermodynamic equilibrium in the system (e.g., GHIORSO, 1985; GHIORSO and KELEMEN, 1987; GHIORSO and SACK, 1994). The algorithm described here could be used to calculate the energetic drive for crystal growth in magmatic systems (GHIORSO, 1987) or be utilized to estimate the driving force for crystal dissolution reactions. Compared to previous algorithms proposed for computing the saturation condition of multicomponent solids precipitating from aqueous solutions (REED, 1982; HARVEY et al., 1987) or silicate liquids (GHIORSO, 1985), the proposed algorithm is the only one that returns directly the chemical affinity of the disequilibrium process. When timed against the algorithm of GHIORSO (1985) on identical problems, the algorithm proposed here is about an order of magnitude more efficient.

Detection of Instability Within a Homogeneous Phase

In this section, an algorithm is developed to address the question of the thermodynamic stability of a homogeneous phase with respect to unmixing. In the normal practice of computing equilibrium phase proportions by potential minimization techniques, this question arises at the close of every minimization attempt. Some check must be made as to whether, in the course of minimizing the energy of the system and consequently computing the compositions and proportions of the specified phases in the assemblage, the composition of some phase has not inadvertently become metastable.

For example, in computing phase equilibria in magmatic systems, as crystallization proceeds, the liquid composition may evolve so as to become metastable with respect to two coexisting immiscible liquids. Once this metastability is detected, two liquids are specified to the potential minimization procedure, and the process of computing the equilibrium compositions and proportions is repeated. A check for the intrinsic stability of each phase in a computed "equilibrium" assemblage is demanded because algorithms which determine phase proportions and phase compositions by potential minimization techniques, assume that the phase assemblage specified at the onset is the final phase assemblage. These algorithms vary only the proportion and composition of each phase in order to minimize the energy of the system. Because a check for instability must be made for every phase in an assemblage, we require a rapid algorithm that is applicable to phases with highly nonideal Gibbs energy surfaces. The algorithm presented here meets this challenge.

The procedure is developed by describing first a two-component example, then a three-component example, and finally by stating the general algorithm. Consider a two-component regular solution with an interaction parameter of 20 kJ at a temperature of 1000 K. Recall that this model was utilized as an example for the previous algorithm and that the molar Gibbs free energy of mixing of this solution is plotted in Fig. 2. The minima in \bar{G}^{mix} are located at X -values of 0.1692 and 0.8308. Any composition interior to this interval is metastable with respect to unmixing. Suppose a tangent line is drawn to the \bar{G}^{mix} curve at the point 0.1692. This line is obviously horizontal and intersects the \bar{G}^{mix} curve at the other minimum. Now, we subtract the Gibbs energy given by this tangent line from \bar{G}^{mix} . The result, $\Delta\bar{G}$, is plotted as the heavy curve in Fig. 4. Note that this new curve simply represents the original \bar{G}^{mix} function translated so that the minima now occur at a $\Delta\bar{G}$ value of zero. Next, consider constructing a tangent line to the \bar{G}^{mix} curve at some smaller

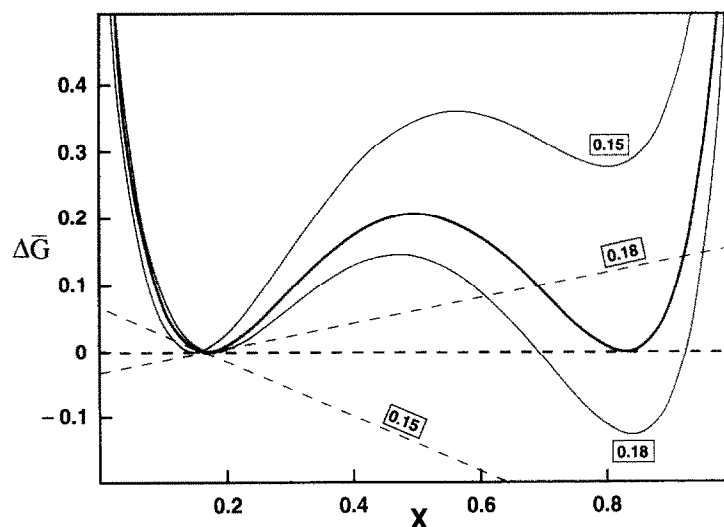


FIG. 4. Plot of the function defined by Eqn. 15 for a binary regular solution (W equal 20 kJ, T equal 1000 K) with a reference composition (X_0) chosen at three points of tangency: X equal to 0.15 (outside the solvus), X equal to 0.1692 (along one limb of the solvus), and X equal to 0.18 (within the solvus). The dashed lines correspond to the orientation of the tangent line with respect to the molar Gibbs free energy of mixing curve at the indicated composition.

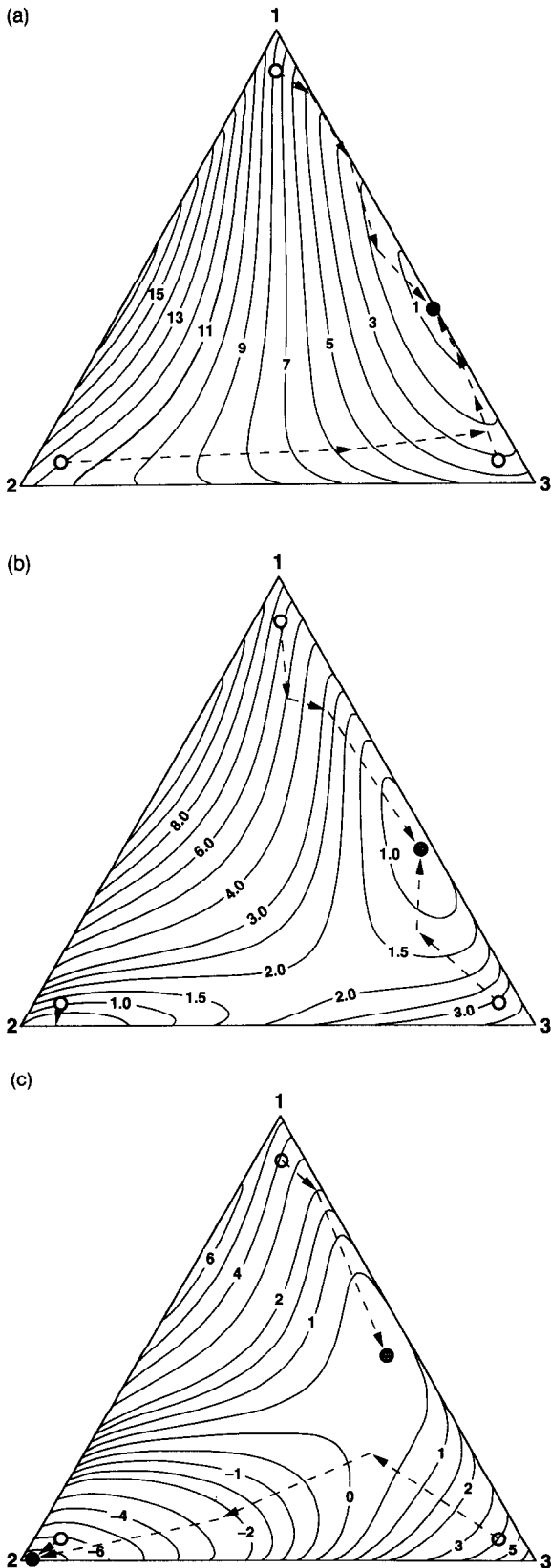


FIG. 5. Contour diagrams of the function $\Delta\bar{G}$ (Eqn. 15) for a three-component regular solution with W_{12} , W_{13} , and W_{23} chosen to be 50, 0, and 20 kJ, respectively. Contours are in kJ. The temperature is assumed to be 1000 K. Reference compositions are denoted by the horizontally ruled dot along the 1–3 join and are given by

X -value, say 0.15. If the Gibbs energy values given by this tangent line are subtracted from \bar{G}^{mix} , the result is the $\Delta\bar{G}$ vs. X curve labeled 0.15 in Fig. 4. The equivalently labeled dashed line in Fig. 4 indicates the orientation of the tangent line with respect to \bar{G}^{mix} . The same procedure may be applied to a tangent line of the \bar{G}^{mix} curve at some X value inside the metastable region, say 0.18. The resulting $\Delta\bar{G}$ function is also plotted in Fig. 4. Notice that the function $\Delta\bar{G}(0.15)$ is greater than or equal to zero for all X , whereas the function $\Delta\bar{G}(0.18)$ is negative at large X . This result can be generalized to the rule that $\Delta\bar{G}$ will always be greater than or equal to zero if the tangent line is evaluated outside the metastable region, and it will be somewhere less than zero if the tangent line is evaluated inside the metastable region. This rule suggests an algorithm for detecting instability.

Consider the result of minimizing a particular function $\Delta\bar{G}$, which has been constructed at a point of tangency corresponding to some composition of unknown stability. If we choose as an initial guess for the minimization algorithm some composition very close to X equal to zero or one, the procedure will locate either the left or right minimum of $\Delta\bar{G}$. If the minimization is performed twice, once with each of these initial guesses, both minima will be found. One of the two minima identified by the procedure must be located at the point of tangency, i.e., the initial composition being investigated for stability (see Fig. 4). That minimum may be discarded from consideration. If the function value of $\Delta\bar{G}$ at the other minimum is positive, the composition under investigation is stable. If it is negative, the composition specifying the point of tangency is metastable, and will most likely unmix to a second phase with a composition given approximately by the location of this second minimum. Let us see how this approach works in a three-component system.

Assuming the composition (X_1, X_2) equal to (0.30, 0.01) and the Gibbs free energy of mixing surface plotted in Fig. 3a, a tangent plane may be constructed to the Gibbs surface at this composition, and a function $\Delta\bar{G}$ evaluated in a manner analogous to the binary. A contoured surface of this function is plotted in Fig. 5a. Utilizing this diagram, the question may be asked: is the composition (0.30, 0.01) metastable? The method to answer this question, as deduced from the previous example, is to locate the minima of $\Delta\bar{G}$, discard the minimum corresponding to the original composition, and evaluate the sign of the function for the remainder. A glance at Fig. 5a reveals that the only minimum in $\Delta\bar{G}$ is at the composition of tangency; hence, this composition is stable. Formally, this fact could be deduced by performing three separate minimizations of the function $\Delta\bar{G}$, starting each time with a different initial guess. Suitable choices are indicated by the open dots in Fig. 5a, and correspond to compositions very close to each of the three endmember components in the system. The computed descent paths to the minimum are indicated on Fig. 5. These were obtained using Algorithm No. 21

(X_1, X_2) equal to (0.30, 0.01) in (a), (0.300, 0.0522) in (b), and (0.3, 0.1) in (c), corresponding to outside, on, and interior to the solvus limb. The open dots denote initial guesses for an algorithm whose objective is to find the minima in $\Delta\bar{G}$. Dashed lines and arrows describe the path to the descent to the minimum. The horizontally ruled dot near the 2-apex in (c) denotes the global minimum in $\Delta\bar{G}$.

(*Variable metric minimiser*) of NASH (1990). In all three cases, the single minimum is located numerically and we deduce that the original composition is stable.

Now consider the reference composition (0.300, 0.0522) which happens to correspond to a point on the limb of the solvus in this system. The $\Delta\bar{G}$ function for this case is contoured in Fig. 5b. Note that there are now two minima in $\Delta\bar{G}$ and that both minima occur at exact zeroes of the function. These two minima define the orientation of a tie line across the solvus. These minima may be located by starting from the same three initial guesses as before. The starting points near 1 and 3 result in finding the initial point of tangency. From the point near 2, the minimizer descends directly to the other minimum and we conclude that the initial composition is incipiently unstable. Finally, consider the reference composition given by (0.3, 0.1) and the corresponding $\Delta\bar{G}$ function contoured in Fig. 5c. Once again, there are two minima in $\Delta\bar{G}$, but the one closest to pure 2 is in this case located at strongly negative values of the function: the initial composition is well within the solvus and is metastable. Two of the three initial guesses result in locating the deep minimum near 2 and one permits descent to the initial composition at the point of tangency. We conclude that the original composition is metastable and deduce from Fig. 5c the approximate solvus extent and tie line orientation for the equilibrium two-phase assemblage.

Based upon our analysis of the two and three-component cases, the following general algorithm may be stated.

Algorithm for the detection of thermodynamic instability in a phase, at some specified temperature and pressure

(step 0a) Specify a model for the molar Gibbs free energy of mixing of an $n + 1$ component solution in terms of n independent compositional variables r_1, r_2, \dots, r_n (arranged as the elements of a vector, \vec{r}). T and P . Note that analytical expressions for the first compositional derivative of this function are utilized in this algorithm. See the appendix for general methods of obtaining these derivatives.
(step 0b) Specify the reference composition, \vec{r}_0 , of the phase.

(step 1) Compute the function

$$\Delta\bar{G}(\vec{r}) = \bar{G}^{\text{mix}}(\vec{r}) - \left[\bar{G}^{\text{mix}}(\vec{r}_0) + \sum_{i=1}^n \frac{\partial \bar{G}^{\text{mix}}}{\partial r_i} \bigg|_{\vec{r}_0} (\vec{r} - \vec{r}_0) \right], \quad (15)$$

which represents the difference between the molar Gibbs free energy of mixing and a tangent hypersurface to \bar{G}^{mix} at \vec{r}_0 .

(step 2) Let the $n + 1$ endmember components in the solid solution be indexed on i , and let X_1, \dots, X_{n+1} denote the mole fractions of these endmembers. Let i equal 1:

(step 2.1) Compute a composition \vec{X}_{in} (i.e. $[X_1, X_2, \dots, X_n, X_{n+1}]_{\text{in}}$) such that

$$X_i = \frac{10(n+1)}{10(n+1) + n} \quad \text{and} \quad X_{j \neq i} = \frac{1}{10(n+1) + n}.$$

Transform the result (if a component transformation is necessary) into the initial guess \vec{r}_{in} .

(step 2.2) Minimize the function $\Delta\bar{G}$ given by Eqn. (15) with respect to \vec{r} . Use \vec{r}_{in} as an initial guess for the minimum. Algorithm No. 21 of NASH (1990, *Variable metric minimizer*) is ideally suited to this task. It requires only first derivatives of the function and incorporates a provision to keep the solution vector within bounds during the course of minimization. Call the location of the minimum \vec{r}_{min} .

(step 2.3) If \vec{r}_{min} is "sufficiently" close to \vec{r}_0 , that is if the dot product $\vec{r}_{\text{min}}^1 \vec{r}_0$ is less than some acceptable tolerance, then the minimization routine has found the original point of tangency. Proceed to step 2.6.

(step 2.4) If $\Delta\bar{G}(\vec{r}_{\text{min}})$ is greater than zero, then the minimization routine has determined that a miscibility gap exists, but the reference point \vec{r}_0 is outside this gap. Proceed to step 2.6.

(step 2.5) If $\Delta\bar{G}(\vec{r}_{\text{min}})$ is less than or equal to zero, then the reference composition \vec{r}_0 is unstable with respect to unmixing. The approximate tie-line is given by the vector $\vec{r}_0 - \vec{r}_{\text{min}}$. The accuracy of this approximation worsens as $\Delta\bar{G}(\vec{r}_{\text{min}})$ becomes more negative; it is exact if $\Delta\bar{G}(\vec{r}_{\text{min}})$ is zero. In any event, \vec{r}_{min} provides an excellent initial guess for the composition of the second phase, if one is required for some potential minimization procedure.

(step 2.6) Increment i . If $i > n + 1$, then exit the algorithm. Otherwise, go to step 2.1.

The above algorithm has been implemented in the C programming language and has proved successful in detecting instability in phases with up to twelve components. In practice, the procedure will occasionally find the location of more than one minimum with negative function values, indicating that the initial composition is unstable with respect to unmixing into more than two phases. It is found that the best way to proceed in this eventuality is to add one phase at a time to the specified list of stable phases in the assemblage, choosing the \vec{r}_{min} which gives the most negative value of $\Delta\bar{G}$ from the list of likely compositions. At this point, potential function minimization techniques are used to determine the actual compositions and proportions of the coexisting phases, and the instability algorithm is invoked again. Further instability, if detected, is similarly dealt with by adding one new phase at a time. This procedure is numerically stable and affords the possibility of detecting up to $n + 1$ coexisting immiscible phases from an $n + 1$ component model function.

SUMMARY

Two algorithms are developed which address critical aspects of the calculation of equilibrium phase relations in highly nonideal thermodynamic systems. The first deals with detection of the saturation state of a phase and the second addresses the issue of the intrinsic stability of a phase with respect to unmixing. Both algorithms have been implemented

in C and tested with complex solution models describing solid and liquid phases in magmatic systems (GHIORSO and SACK, 1994). The algorithms are intended to support potential function minimization techniques and are designed for rapid and repeated execution within a generalized modeling code.

Acknowledgments—Support for this investigation was provided by external research funding and a generous equipment grant from Digital Equipment Corporation. Careful reviews by Professor Jim Nicholls and an anonymous reviewer helped improve the presentation.

Editorial handling: P. C. Hess

REFERENCES

- BARRON L. M. (1978) The geometry of multicomponent exsolution. *Amer. J. Sci.* **278**, 1269–1306.
- DARKEN L. S. and GURRY R. W. (1953) *Physical Chemistry of Metals*. McGraw Hill.
- GHIORSO M. S. (1985) Chemical mass transfer in magmatic processes I. Thermodynamic relations and numerical algorithms. *Contrib. Mineral. Petrol.* **90**, 107–120.
- GHIORSO M. S. (1987) Chemical mass transfer in magmatic processes. III. Crystal growth, chemical diffusion and thermal diffusion in multicomponent silicate melts. *Contrib. Mineral. Petrol.* **96**, 291–313.
- GHIORSO M. S. (1990a) Thermodynamic properties of hematite-ilmenite-geikielite solid solutions. *Contrib. Mineral. Petrol.* **104**, 645–667.
- GHIORSO M. S. (1990b) The application of the Darken equation to mineral solid solutions with variable degrees of order-disorder. *Amer. Mineral.* **75**, 539–543.
- GHIORSO M. S. and KELEMEN P. B. (1987) Evaluating reaction stoichiometry in magmatic systems evolving under generalized thermodynamic constraints: Examples comparing isothermal and isenthalpic assimilation. In *Magmatic Processes: Physicochemical Principles* (ed. B. O. MYSEN); *Geochem. Soc. Sp. Publ. 1*, pp. 319–336.
- GHIORSO M. S. and SACK R. O. (1994) Chemical mass transfer in magmatic processes. IV. A revised and internally consistent thermodynamic model for the interpolation and extrapolation of liquid-solid equilibria in magmatic systems at elevated temperatures and pressures. *Contrib. Mineral. Petrol.* (in press).
- HARVIE C. E., GREENBERG J. P., and WEARE J. H. (1987) A chemical equilibrium algorithm for highly nonideal multiphase systems: Free energy minimization. *Geochim. Cosmochim. Acta* **51**, 1045–1057.
- HIRSCHMANN M. (1991) Thermodynamics of multicomponent olivines and the solution properties of (Ni, Mg, Fe)₂SiO₄ and (Ca, Mg, Fe)₂SiO₄ olivines. *Amer. Mineral.* **76**, 1232–1248.
- NASH J. C. (1990) *Compact Numerical Methods for Computers*, 2nd edition. Adam Hilger.
- REED M. H. (1982) Calculation of multicomponent chemical equilibrium and reaction processes in systems involving minerals, gases, and an aqueous phase. *Geochim. Cosmochim. Acta* **46**, 513–528.
- SACK R. O. and GHIORSO M. S. (1989) Importance of considerations of mixing properties in establishing an internally consistent thermodynamic database: Thermochemistry of minerals in the system Mg₂SiO₄–Fe₂SiO₄–SiO₂. *Contrib. Mineral. Petrol.* **102**, 41–68.
- SACK R. O. and GHIORSO M. S. (1991a) An internally consistent model for the thermodynamic properties of Fe-Mg-titanomagnetite-aluminate spinels. *Contrib. Mineral. Petrol.* **106**, 474–505.
- SACK R. O. and GHIORSO M. S. (1991b) Chromian spinels as petrogenetic indicators: Thermodynamics and petrological applications. *Amer. Mineral.* **76**, 827–847.
- SACK R. O. and GHIORSO M. S. (1994a) Thermodynamics of multicomponent pyroxenes: I. Formulation of a general model. *Contrib. Mineral. Petrol.* **116**, 277–286.
- SACK R. O. and GHIORSO M. S. (1994b) Thermodynamics of multicomponent pyroxenes: II. Applications to phase relations in the quadrilateral. *Contrib. Mineral. Petrol.* **116**, 287–300.
- SACK R. O. and GHIORSO M. S. (1994c) Thermodynamics of multicomponent pyroxenes: III. Calibration of Fe²⁺(Mg)₋₁, TiAl₂(MgSi₂)₋₁, TiFe³⁺(MgSi₂)₋₁, AlFe³⁺(MgSi)₋₁, NaAl-(CaMg)₋₁, Al₂(MgSi)₋₁ and Ca(Mg)₋₁ exchange reactions between pyroxenes and silicate melts. *Contrib. Mineral. Petrol.* (in press).
- SMITH W. R. and MISSEN R. W. (1982) *Chemical Reaction Equilibrium Analysis*. Wiley.
- THOMPSON J. B., JR. (1969) Chemical reactions in crystals. *Amer. Mineral.* **54**, 341–375.
- THOMPSON J. B., JR. (1970) Chemical reactions in crystals: Corrections and clarification. *Amer. Mineral.* **55**, 528–532.

APPENDIX

Summary of the Numerical Method for Solving the System of Simultaneous Nonlinear Equations

The nonlinear system embodied in Eqn. 5 may be efficiently solved using Marquardt's method as modified by NASH (1990) for bounded feasible solution domains. We define functions $\varphi_j(r_1, r_2, \dots, r_n, A, T, P)$ in terms of the right-hand sides of each of the $n + 1$ equations in (5)

$$\varphi_j = \mu_j^{\text{sol}} - A - \sum_{i=1}^n \nu_{ji} \mu_i^{\text{liq}}, \quad (\text{A1-1})$$

and form the sum of squares of these quantities:

$$\Phi = \sum_{j=1}^{n+1} \varphi_j^2. \quad (\text{A1-2})$$

The minimum of Φ with respect to the n -elements of \vec{r} and the scalar A is determined at constant temperature and pressure by choosing an appropriate initial guess (\vec{r}_0 and A_0) to the solution and expanding Φ in a Taylor series in the vector \vec{q} , defined by:

$$\vec{q} = \begin{bmatrix} \vec{r} \\ A \end{bmatrix} - \begin{bmatrix} \vec{r}_0 \\ A_0 \end{bmatrix}. \quad (\text{A1-3})$$

Certain simplifying assumptions are employed in constructing the Taylor series. The series is truncated to second order in \vec{q} , i.e.,

$$\Phi(\vec{q}) \approx \Phi_0 + \vec{\varphi}_0^T J_0 \vec{q} + \frac{\vec{q}^T J_0^T J_0 \vec{q}}{2} \quad (\text{A1-4})$$

and the quadratic term is approximated from the Jacobian of the nonlinear system:

$$\frac{\partial^2 \Phi}{\partial \begin{bmatrix} \vec{r} \\ A \end{bmatrix}^2} \approx J^T J, \quad (\text{A1-5})$$

where the Jacobian is given by

$$J = \begin{bmatrix} \frac{\partial \varphi_1}{\partial r_1} & \dots & \frac{\partial \varphi_1}{\partial r_n} & \frac{\partial \varphi_1}{\partial A} \\ \vdots & \ddots & \vdots & \vdots \\ \frac{\partial \varphi_{n+1}}{\partial r_1} & \dots & \frac{\partial \varphi_{n+1}}{\partial r_n} & \frac{\partial \varphi_{n+1}}{\partial A} \end{bmatrix}. \quad (\text{A1-6})$$

Equations A1-4 and A1-5 are valid if the initial guess is a good approximation to the actual solution. The partial derivatives in the Jacobian matrix may be readily evaluated from Eqn. A1-1:

$$\frac{\partial \varphi_j(r_1, \dots, r_n, A)}{\partial r_k} = (\mu_j^{\text{sol}} - A - \sum_{i=1}^n \nu_{ji} \mu_i^{\text{liq}}) \frac{\partial \mu_j^{\text{sol}}}{\partial r_k}$$

$$\frac{\partial \varphi_j(r_1, \dots, r_n, A)}{\partial A} = -(\mu_j^{\text{sol}} - A - \sum_{i=1}^n \nu_{ji} \mu_i^{\text{liq}}). \quad (\text{A1-7})$$

A method for obtaining the compositional derivatives of the solid chemical potentials is discussed in the next section. The process is not straightforward if the solid demonstrates compositionally dependent atomic ordering.

A minimum of Eqn. A1-4 is obtained by setting the derivative to zero and solving for the "correction"-term, \vec{q} :

$$\frac{d\Phi(\vec{q})}{d\vec{q}} = 0 \Rightarrow J_0^T J_0 \vec{q} = -J_0^T \vec{\varphi}_0. \quad (\text{A1-8})$$

In practice, if the matrix product $J_0^T J_0$ is not positive definite or if the derived vector \vec{q} renders the solution vector $\begin{bmatrix} \vec{r} \\ A \end{bmatrix}$ unfeasible, then

Eqn. A1-8 is modified by introducing an arbitrary positive constant λ according to:

$$(J_0^T J_0 + \lambda I) \vec{q} = -J_0^T \vec{\varphi}_0, \quad (\text{A1-9})$$

where I is the identity matrix. This constant is referred to as the Marquardt parameter. The correction vector resulting from solution of Eqn. A1-9 is used to construct an estimate of the solution of the nonlinear system by application of Eqn. A1-3. This estimate becomes the new initial guess of a subsequent iteration. The process is repeated until the norm of the correction vector is "zero." At the global minimum of Eqn. A1-2, both Φ and the Marquardt parameter should have a value of zero.

Evaluation of the Equilibrium Thermodynamic Properties of Phases with Variable Degrees of Microscopic Order

The algorithms discussed in this paper require the evaluation of compositional derivatives of the Gibbs free energy and of the chemical potentials of endmember components of the solid phases. Obtaining analytical expressions for these derivatives is complicated by the fact that the energetic description of the solid is often written in terms of one or more ordering parameters which describe the state of atomic order/disorder in the crystal (THOMPSON, 1969, 1970). If the solid is in a state of internal or homogeneous equilibrium, these ordering parameters are a unique function of composition, T and P , and the derivatives of interest may be completely determined. In this appendix, we summarize a method for obtaining these derivatives.

In general, the molar Gibbs free energy of a solid solution, \bar{G} , may be expressed in terms of a vector of independent compositional variables, \vec{r} , a vector of ordering parameters, \vec{s} , the temperature, T , and the pressure, P , i.e., $\bar{G}(\vec{r}, \vec{s}, T, P)$. \bar{G} is an intensive thermodynamic quantity and may always be related to the extensive Gibbs free energy of solution by multiplication of the total number of moles of the phase in the system, η :

$$G(\eta, \vec{r}, \vec{s}, T, P) = \eta \bar{G}(\vec{r}, \vec{s}, T, P). \quad (\text{A2-1})$$

It should be noted that the relation embodied in Eqn. A2-1 affords the basis of transforming any derivative of \bar{G} into a corresponding derivative of G . We simply write down expressions for the total derivatives of G :

$$dG = \eta d\bar{G} + \bar{G} d\eta, \quad (\text{A2-2})$$

$$d^2 G = \eta d^2 \bar{G} + 2 d\eta d\bar{G} + \bar{G} d^2 \eta, \quad (\text{A2-3})$$

and specify them for the parameter of interest, i.e., Eqn. A2-2 may be used to "derive"

$$\frac{\partial G}{\partial T} = \eta \frac{\partial \bar{G}}{\partial T} + \bar{G} \frac{\partial \eta}{\partial T} = \eta \frac{\partial \bar{G}}{\partial T},$$

since the total number of moles of the phase is independent of temperature. It follows from Eqns. A2-1 through A2-3 that we need only focus our attention on derivatives of \bar{G} .

In practice, \bar{G} is often modeled as the sum of a configurational entropy contribution and a truncated second-order Taylor expansion in the composition and ordering variables:

$$\begin{aligned} \bar{G}(\vec{r}, \vec{s}, T, P) = & -TS^{\text{conf}}(\vec{r}, \vec{s}) + \bar{G}_0(T, P) + \sum_{i=1}^n \bar{G}_{r_i} r_i + \sum_{i=1}^m \bar{G}_{s_i} s_i \\ & + \sum_{i=1}^n \sum_{j=1}^n \bar{G}_{r_i r_j} r_i r_j + \sum_{i=1}^n \sum_{j=1}^m \bar{G}_{r_i s_j} r_i s_j + \sum_{i=1}^m \sum_{j=1}^m \bar{G}_{s_i s_j} s_i s_j, \end{aligned} \quad (\text{A2-4})$$

where r_i denotes one of the n -elements of \vec{r} and s_i refers to one of the m -elements of \vec{s} . This formulation is highly successful in describing extremely nonideal solid solutions (GHIORSO, 1990a; HIRSCHMANN, 1991; SACK and GHIORSO, 1989, 1991a,b, 1994a,b,c). It should be remarked that Eqn. A2-4 is a formulation of the molar Gibbs free energy which is applicable to an arbitrary (in general a disequilibrium) state of order. As the higher order Taylor expansion coefficients are usually taken to be constants, it is a straightforward matter to evaluate analytically partial derivatives of Eqn. A2-4, with respect \vec{r} , \vec{s} , T or P . Thus, expressions like Eqn. A2-4 may be manipulated in conjunction with the generalized form of Darken's relation (GHIORSO, 1990b)

$$\mu_i = \bar{G} + \sum_{j=1}^n f_j(r_j) \frac{\partial \bar{G}}{\partial r_j} + \sum_{j=1}^m g_j(s_j) \frac{\partial \bar{G}}{\partial s_j}, \quad (\text{A2-5})$$

to provide algebraic expressions for the chemical potentials of endmember solid components. The functions f_j and g_j in Eqn. A2-5 are determined by the stoichiometry of the endmember component (GHIORSO, 1990b).

Let us focus on deriving expressions for the compositional derivatives of these endmember chemical potentials, specifically, derivatives which are appropriate for the algorithms presented in this paper and represent variation of the chemical potential in an equilibrium state of internal order. The methods employed will be generally applicable to any \vec{r} , T , or P derivative of μ_i or \bar{G} that may be required.

From Eqn. A2-5, the total derivative of μ_i may be written (assuming constant T and P):

$$\begin{aligned} d\mu_i = & d\bar{G} + \sum_{j=1}^n \left[df_j(r_j) \frac{\partial \bar{G}}{\partial r_j} + f_j(r_j) d\left(\frac{\partial \bar{G}}{\partial r_j}\right) \right] \\ & + \sum_{j=1}^m \left[dg_j(s_j) \frac{\partial \bar{G}}{\partial s_j} + g_j(s_j) d\left(\frac{\partial \bar{G}}{\partial s_j}\right) \right]. \end{aligned} \quad (\text{A2-6})$$

We specify Eqn. A2-6 to reflect the total derivative of μ_i , with respect to an infinitesimal variation of the k^{th} element of \vec{r} :

$$\begin{aligned} \frac{d\mu_i}{dr_k} = & \frac{d\bar{G}}{dr_k} + \frac{df_j(r_k)}{dr_k} \frac{\partial \bar{G}}{\partial r_k} + \sum_{j=1}^n f_j(r_j) \frac{d\left(\frac{\partial \bar{G}}{\partial r_j}\right)}{dr_k} \\ & + \sum_{j=1}^m g_j(s_j) \frac{d\left(\frac{\partial \bar{G}}{\partial s_j}\right)}{dr_k}. \end{aligned} \quad (\text{A2-7})$$

Note that Eqn. A2-7 has been simplified by recognizing that the elements of \vec{r} are independent, i.e., $\frac{df_j(r_j)}{dr_k} = 0$ for $j \neq k$, and that the ordering state in the general (disequilibrium) case is not a function of composition, i.e., $\frac{dg_i(s_j)}{dr_k} = 0$. This is an extremely convenient result, but implies that the derivative defined by Eqn. A2-7 needs yet to be projected to, or evaluated for, the equilibrium ordering state. Given that the total derivative of \bar{G} may be expressed as

$$d\bar{G} = \sum_{j=1}^n \frac{\partial \bar{G}}{\partial r_j} dr_j + \sum_{j=1}^m \frac{\partial \bar{G}}{\partial s_j} ds_j - \bar{S} dT + \bar{V} dP, \quad (\text{A2-8})$$

we obtain the first term on the right-hand side (rhs) of Eqn. A2-7:

$$\frac{d\bar{G}}{dr_k} = \frac{\partial \bar{G}}{\partial r_k} + \sum_{j=1}^m \frac{\partial \bar{G}}{\partial s_j} \frac{ds_j}{dr_k}. \quad (\text{A2-9})$$

Writing $d\left(\frac{\partial \bar{G}}{\partial r_j}\right)$ and $d\left(\frac{\partial \bar{G}}{\partial s_j}\right)$ in a manner similar to Eqn. A2-8 and proceeding to specify this quantity for dr_k , yields

$$\frac{d\left(\frac{\partial \bar{G}}{\partial r_j}\right)}{dr_k} = \frac{\partial^2 \bar{G}}{\partial r_j \partial r_k} + \sum_{l=1}^m \frac{\partial^2 \bar{G}}{\partial r_j \partial s_l} \frac{ds_l}{dr_k} \quad (\text{A2-10})$$

and

$$\frac{d\left(\frac{\partial \bar{G}}{\partial s_j}\right)}{dr_k} = \frac{\partial^2 \bar{G}}{\partial r_k \partial s_j} + \sum_{l=1}^m \frac{\partial^2 \bar{G}}{\partial s_j \partial s_l} \frac{ds_l}{dr_k} \quad (\text{A2-11})$$

Thus, all the total derivatives on the rhs of Eqn. A2-7 may be expressed, using Eqns. A2-9, A2-10, and A2-11, in terms of simple partial derivatives and the total derivative matrix, $\frac{d\bar{s}}{d\bar{r}}$. The requisite partial derivatives may be computed directly from the definition of \bar{G} . The total derivative matrix, $\frac{d\bar{s}}{d\bar{r}}$, is undefined unless a relationship is specified between ordering state and composition. The natural relation is the requirement of internal or homogeneous equilibrium.

The condition of homogeneous equilibrium is specified by setting the vector $\frac{\partial \bar{G}}{\partial \bar{s}}$ equal to zero. This is the mathematical consequence of the stipulation that the Gibbs free energy must be minimal, with respect to variation of the ordering parameter(s), if the phase is in a state of homogeneous equilibrium. Writing this condition out explicitly,

$$\begin{bmatrix} \frac{\partial \bar{G}}{\partial s_1} \\ \vdots \\ \frac{\partial \bar{G}}{\partial s_m} \end{bmatrix} = \begin{bmatrix} 0 \\ \vdots \\ 0 \end{bmatrix} = \begin{bmatrix} \varphi_1(\bar{r}, \bar{s}_{\text{eq}}, T, P) \\ \vdots \\ \varphi_m(\bar{r}, \bar{s}_{\text{eq}}, T, P) \end{bmatrix}, \quad (\text{A2-12})$$

demonstrates that the problem involved in computing equilibrium values of \bar{s} is really one of solving m nonlinear equations in m unknowns. The unknowns are the m -elements of $\bar{s}_{\text{eq}}(\bar{r}, T, P)$. Equation A2-12 is usually solved using Newton's method (NASH, 1990). Now,

let us consider the j^{th} element of the vector $\frac{\partial \bar{G}}{\partial \bar{s}} \Big|_{\bar{s}_{\text{eq}}}$, where the vertical

line implies evaluation of the quantity to the left of the line at the "point" specified on the right. We can write the total derivative in the usual manner:

$$d\left(\frac{\partial \bar{G}}{\partial s_j}\right) \Big|_{\bar{s}_{\text{eq}}} = \sum_{l=1}^n \frac{\partial^2 \bar{G}}{\partial r_l \partial s_j} \Big|_{\bar{s}_{\text{eq}}} dr_l \Big|_{\text{eq}} + \sum_{l=1}^m \frac{\partial^2 \bar{G}}{\partial s_j \partial s_l} \Big|_{\bar{s}_{\text{eq}}} ds_l \Big|_{\text{eq}} + \frac{\partial^2 \bar{G}}{\partial T \partial s_j} \Big|_{\bar{s}_{\text{eq}}} dT \Big|_{\text{eq}} + \frac{\partial^2 \bar{G}}{\partial P \partial s_j} \Big|_{\bar{s}_{\text{eq}}} dP \Big|_{\text{eq}}. \quad (\text{A2-13})$$

The left-hand side of Eqn. A2-13 is zero. This is because any variation of $\frac{\partial \bar{G}}{\partial s_j} \Big|_{\bar{s}_{\text{eq}}}$ is zero since $\frac{\partial \bar{G}}{\partial \bar{s}} \Big|_{\bar{s}_{\text{eq}}}$ is constant (and also happens to be equal to zero) in the equilibrium ordering state. Evaluating the lhs of Eqn. A2-13 at constant T and P for an infinitesimal change in r_k yields:

$$0 = \frac{\partial^2 \bar{G}}{\partial r_k \partial s_j} \Big|_{\bar{s}_{\text{eq}}} + \sum_{l=1}^m \frac{\partial^2 \bar{G}}{\partial s_j \partial s_l} \Big|_{\bar{s}_{\text{eq}}} \frac{ds_l}{dr_k} \Big|_{\text{eq}}, \quad (\text{A2-14})$$

which is a linear equation in $\frac{ds_1}{dr_k} \Big|_{\text{eq}}, \frac{ds_2}{dr_k} \Big|_{\text{eq}}, \dots, \frac{ds_m}{dr_k} \Big|_{\text{eq}}$. We may combine statements of Eqn. A2-14 for all n elements of \bar{r} and all m elements of \bar{s} into a matrix equation:

$$-\begin{bmatrix} \frac{\partial^2 \bar{G}}{\partial r_1 \partial s_1} & \dots & \frac{\partial^2 \bar{G}}{\partial r_n \partial s_1} \\ \vdots & \ddots & \vdots \\ \frac{\partial^2 \bar{G}}{\partial r_1 \partial s_m} & \dots & \frac{\partial^2 \bar{G}}{\partial r_n \partial s_m} \end{bmatrix} \Big|_{\bar{s}_{\text{eq}}} \begin{bmatrix} ds_1 \Big|_{\text{eq}} \\ \vdots \\ ds_m \Big|_{\text{eq}} \end{bmatrix} = \begin{bmatrix} \frac{\partial^2 \bar{G}}{\partial s_1 \partial s_1} & \dots & \frac{\partial^2 \bar{G}}{\partial s_m \partial s_1} \\ \vdots & \ddots & \vdots \\ \frac{\partial^2 \bar{G}}{\partial s_1 \partial s_m} & \dots & \frac{\partial^2 \bar{G}}{\partial s_m \partial s_m} \end{bmatrix} \Big|_{\bar{s}_{\text{eq}}} \begin{bmatrix} ds_1 \Big|_{\text{eq}} \\ \vdots \\ ds_m \Big|_{\text{eq}} \end{bmatrix} \quad (\text{A2-15})$$

Equation A2-15 may be used to solve for the elements of the matrix $\frac{d\bar{s}}{d\bar{r}} \Big|_{\text{eq}}$ in the particular case of homogeneous equilibrium. Note that

a solution for $\frac{d\bar{s}}{d\bar{r}} \Big|_{\text{eq}}$ is always possible, since the matrix of second-partial derivatives, $\frac{\partial^2 \bar{G}}{\partial \bar{s} \partial \bar{s}} \Big|_{\bar{s}_{\text{eq}}}$, is guaranteed to have an inverse; it must

be positive definite since the Gibbs energy is minimal in the equilibrium ordering state.

All of these results may be assembled to rewrite Eqns. A2-5, A2-7, A2-9, A2-10, and A2-11 in the equilibrium ordering state. Equation A2-5 becomes:

$$\mu_i^{\text{eq}} = \bar{G} \Big|_{\bar{s}_{\text{eq}}} + \sum_{j=1}^n f_j(r_j) \frac{\partial \bar{G}}{\partial r_j} \Big|_{\bar{s}_{\text{eq}}}, \quad (\text{A2-5 eq})$$

since all the elements of $\frac{\partial \bar{G}}{\partial \bar{s}} \Big|_{\bar{s}_{\text{eq}}}$ are zero. Numerical values of \bar{s}_{eq} are computed by solution of Eqn. A2-12. Similarly, Eqn. A2-7 becomes:

$$\frac{d\mu_i}{dr_k} \Big|_{\text{eq}} = \frac{d\bar{G}}{dr_k} \Big|_{\text{eq}} + \frac{df_i(r_k)}{dr_k} \frac{\partial \bar{G}}{\partial r_k} \Big|_{\bar{s}_{\text{eq}}} + \sum_{j=1}^n f_j(r_j) \frac{d\left(\frac{\partial \bar{G}}{\partial r_j}\right)}{dr_k} \Big|_{\bar{s}_{\text{eq}}} + \sum_{j=1}^m g_j(s_j, \text{eq}) \frac{d\left(\frac{\partial \bar{G}}{\partial s_j}\right)}{dr_k} \Big|_{\bar{s}_{\text{eq}}} \quad (\text{A2-7 eq})$$

and Eqns. A2-9 through A2-11 simplify to:

$$\frac{d\bar{G}}{dr_k} \Big|_{\text{eq}} = \frac{\partial \bar{G}}{\partial r_k} \Big|_{\bar{s}_{\text{eq}}}, \quad (\text{A2-9 eq})$$

$$\frac{d\left(\frac{\partial \bar{G}}{\partial r_j}\right)}{dr_k} \Big|_{\text{eq}} = \frac{\partial^2 \bar{G}}{\partial r_j \partial r_k} \Big|_{\bar{s}_{\text{eq}}} + \sum_{l=1}^m \frac{\partial^2 \bar{G}}{\partial r_j \partial s_l} \Big|_{\bar{s}_{\text{eq}}} \frac{ds_l}{dr_k} \Big|_{\text{eq}}, \quad (\text{A2-10 eq})$$

and

$$\frac{d\left(\frac{\partial \bar{G}}{\partial s_j}\right)}{dr_k} \Big|_{\text{eq}} = \frac{\partial^2 \bar{G}}{\partial r_k \partial s_j} \Big|_{\bar{s}_{\text{eq}}} + \sum_{l=1}^m \frac{\partial^2 \bar{G}}{\partial s_j \partial s_l} \Big|_{\bar{s}_{\text{eq}}} \frac{ds_l}{dr_k} \Big|_{\text{eq}}, \quad (\text{A2-11 eq})$$

respectively. The matrix $\frac{d\bar{s}}{d\bar{r}} \Big|_{\text{eq}}$ is obtained by solution of Eqn. A2-15.